

The Luminosity, Colour and Morphology dependence of galaxy filaments in the Sloan Digital Sky Survey Data Release Four

Biswajit Pandey^{*} and Somnath Bharadwaj[†]

Department of Physics and Meteorology

and

Centre for Theoretical Studies

IIT Kharagpur

Pin: 721 302 , India

14 October 2019

ABSTRACT

We have tested for luminosity, colour and morphology dependence of the degree of filamentarity in seven independent nearly two dimensional strips from the Sloan Digital Sky Survey Data Release Four (SDSS DR4). The analysis is carried out at various levels of coarse graining allowing us to address different length-scales. We find that the brighter galaxies have a less filamentary distribution than the fainter ones at all levels of coarse graining. The distribution of red galaxies and ellipticals shows a higher degree of filamentarity compared to blue galaxies and spirals respectively at low levels of coarse graining. The behaviour is reversed at higher levels of coarse graining. We propose a picture where the ellipticals are densely distributed in the vicinity of the nodes where the filaments intersect while the spirals are sparsely distributed along the entire extent of the filaments. Our observations indicate that the regions with an excess of elliptical galaxies are larger than galaxy clusters, protruding into the filaments.

Key words: methods: numerical - galaxies: statistics - cosmology: theory - cosmology: large scale structure of universe

1 INTRODUCTION

One of the most significant aim of all large redshift surveys is to determine the spatial distribution of galaxies in the Universe. Over the last few decades redshift surveys have revealed the large scale structures in the Universe in it's full glory (e.g. , CfA , Geller & Huchra 1989; LCRS, Shectman et al. 1996; 2dFGRS, Colles et al. 2001 and SDSS, Stoughton et al. 2002, Abazajian et al. 2003, Abazajian et al. 2004). It is found that the vast majority of galaxies preferentially reside in an intricate network of interconnected filaments and walls surrounded by voids. The filaments have a dimension of many tens of Mpc in length (Bharadwaj et al. 2004) and 1-2 Mpc in thickness (Ratcliffe et al. 1996, Doroshkevich et al. 2004). In fact the Local Group in which the Milky Way resides, is believed to lie along an extended filament that originates near the Ursa Major and includes both the IC342 and M81 groups and connects with another primary filament which originates from the Virgo cluster and includes the Sculpture group (Peebles, Phelps, Shaya & Tully 2001). The complex filamentary network of galaxies, the so called 'Cosmic web' is possibly the most striking visible feature in the large scale structure of the Universe. Quantifying the Cosmic web and tracing it's origin has remained one of the central issues in cosmology. The analysis of filamentary patterns in the galaxy distribution has a long history dating back to a few papers in the mid-eighties by Zel'dovich , Einasto & Shandarin (1982), Shandarin & Zeldovich (1983) and Einasto et al. (1984). More recently, extensive studies of the LCRS reveal a rich network of interconnected filaments surrounding voids (eg. Shandarin & Yess 1998; Bharadwaj et al. 2000; Müller et al. 2000; Doroshkevich et al. 2001; Trac et al. 2002, Doroshkevich et al. 2004, Bharadwaj et al. 2004, Bharadwaj & Pandey 2004).

* Email: pandey@cts.iitkgp.ernet.in

† Email: somnathb@iitkgp.ac.in

Sheth (2003) has used a technique SURFGEN (Sheth et al. 2003) to study the geometry, topology and morphology of the superclusters in mock SDSS catalogues. Basilakos, Plionis, & Rowan-Robinson (2001) and Kolokotronis, Basilakos, & Plionis (2002) have studied the super-cluster void network in the PSCz and the Abell/ACO cluster catalogue respectively, finding filamentarity to be the dominant feature. Pimblett, Drinkwater & Hawkrigg (2004) have studied the intercluster galaxy filaments in the 2dFGRS.

The Sloan Digital Sky Survey (SDSS) (York et al. 2000) is currently the largest galaxy redshift survey. In a recent paper (Pandey & Bharadwaj 2005) we have analysed the filamentarity in the two equatorial strips of the First Data Release of the SDSS (SDSS DR1). These strips are nearly two dimensional (2-D). We have projected the data onto a plane and analysed the resulting 2-D galaxy distribution. The large volume and dense sampling of the SDSS allows us to construct volume limited subsamples extending over lengthscales which are substantially larger than possible with earlier surveys. We find evidence for connectivity and filamentarity in excess of that of a random point distribution, indicating the existence of an interconnected network of filaments. The filamentarity is found to be statistically significant up to length-scales $80 h^{-1} \text{Mpc}$ and not beyond. Further, we show that the degree of filamentarity exhibits a luminosity dependence with the brighter galaxies having a more concentrated and less filamentary distribution.

It is now quite well accepted that galaxies with different physical properties are differently distributed in space. Studies over several decades have established that ellipticals and spirals are not distributed in the same way. The ellipticals are found predominantly inside regular, rich clusters whereas the field galaxies are mostly spirals. This effect is referred to as ‘‘morphological segregation’’ which has been studied extensively in the literature (eg. Hubble 1936, Zwicky 1968, Davis & Geller 1976, Dressler 1980, Guzzo et al. 1997, Zehavi et al. 2002, Goto et al. 2003). Further, ellipticals exhibit a stronger clustering as compared to spirals (Zehavi et al. 2002). The analysis of the two-point correlation function of galaxies with different colours shows the red galaxies, which are mainly ellipticals with old stellar populations, to have a stronger clustering as compared to the blue galaxies which are mostly spirals (e.g. Willmer, da Costa, & Pellegrini 1998, Brown, Webster, & Boyle 2000, Zehavi et al. 2005). Studies of the topology using the genus statistics show that red galaxies exhibit a shift towards a meatball topology (Hoyle et al. 2002, SDSS EDR, Park et al. 2005, SDSS DR3) implying that they prefer to inhabit the high density environments. It is found that luminous galaxies exhibit a stronger clustering than their fainter counterparts (e.g. Hamilton 1998, Davis et al. 1988, White, Tully & Davis 1988, Park, Vogeley, Geller & Huchra 1994, Loveday, Maddox, Efsthathiou & Peterson 1995, Guzzo et al. 1997, Benoist et al. 1996, Norberg et al. 2001, Zehavi et al. 2005). The difference increase markedly above the characteristic magnitude M^* (Norberg et al. 2001, 2dFGRS, Zehavi et al. 2005, SDSS DR2) of the Schechter luminosity function (Schechter 1976). The detailed luminosity dependence has been difficult to establish because of the limited dynamic range of even the largest redshift surveys.

Einasto et al. (2003) have studied the luminosity distribution of galaxies in high and low density regions of the SDSS to show that brighter galaxies are preferentially distributed in the high density environments. Goto et al. (2003) have studied the morphology density relation in the SDSS(EDR) and found that this relation is less noticeable in the sparsest regions indicating the need for a denser environment for fostering the physical mechanisms responsible for the galaxy morphological changes. Hogg et al. (2003) and Blanton et al. (2003b) find a strong environment dependence for both the colour and luminosity for the SDSS galaxies.

The dependence of clustering on galaxy properties like the luminosity, colour and morphology provides very important inputs for theories of galaxy formation. It is a natural prediction of hierarchical structure formation that the rarer objects which correspond to peaks in the density field should be more strongly clustered than the population itself (Kaiser 1984, Davis et al. 1985, White et al. 1987). A possible interpretation of the observations is that the more luminous galaxies are hosted in higher density peaks as compared to the fainter galaxies. In this scenario the properties of a galaxy are largely decided by the initial conditions at the location where the galaxy is formed. This idea is implemented in the halo model (Jing, Mo & Borner 1998, Benson et al. 2000, Seljak 2000, Peacock & Smith 2000, Ma & Fry 2000, Scoccimarro & Sheth 2001, White et al. 1987, Berlind & Weinberg 2002, Scranton 2002, Yang, Mo & van den Bosch 2003, Yang, Mo, Jing & van den Bosch 2003) where it is postulated that all galaxies lie in virialised halos and the number and type of galaxies in a halo is entirely determined by the halo mass. Cooray & Sheth (2002) provide a detailed review of the halo model. It is well known that galaxy-galaxy interactions and environmental effects are also important in determining the physical properties of a galaxy. For example, ram pressure stripping in galaxy clusters is a possible mechanism for the transformation of a spiral galaxy into an elliptical. Galaxy-galaxy interactions could also provide a mechanism for morphological transformation. In the classical picture galaxies evolve in isolation and morphology is determined at birth, while in the hierarchical model galaxies have no fixed morphology and they can evolve depending on the nature of their mergers. A study of the spatial distribution of different kind of galaxies holds the potential to probe the factors responsible in determining galaxy luminosity, colour and morphology.

Much of the research on the luminosity, morphology and colour dependence of the galaxy distribution has focused either on the morphology segregation in clusters or has studied the behaviour of the two point correlation as a function of these galaxy properties. Filaments are the largest known statistically significant coherent features. They have been shown to be statistically significant to scales as large as $80 h^{-1} \text{Mpc}$. In this paper we study the luminosity, colour and morphology dependence of filaments in the Sloan Digital Sky Survey Data Release Four (SDSS DR4). This allows us to study the distribution of different

types of galaxies on the largest length-scales possible. Such a study will enable us to estimate the length-scale over which the factors responsible for the galaxy segregation operate. While the two-point correlation function completely characterizes the statistical properties of a Gaussian random field, it is well known that the galaxy distribution is significantly non-Gaussian. In fact the presence of large-scale coherent features like filaments is a clear indication of non-Gaussianity. There have been studies of how the three point correlation function depends on galaxy properties (Kayo et al. 2004, Jing & Borner 2004, Gaztañaga et al. 2005). While the first two papers do not find any statistically significant effects, Gaztañaga et al. (2005) find statistically significant colour and luminosity dependence. The present work studies how the largest known non-Gaussian features, the filaments, depend on galaxy properties.

This paper presents progress on many counts compared to our earlier work (Pandey & Bharadwaj 2005) based on the SDSS DR1. The earlier work was restricted to single volume limited subsamples from each of the two equatorial strips. The absolute magnitude range was divided into two equal halves, and these were analysed to test for a luminosity dependence in the filamentarity. For a statistically significant conclusion it is necessary to also estimate the cosmic variance (sample to sample variation) of the filamentarity which was done by bootstrap resampling. We found that the difference in filamentarity between the two magnitude bins was in excess of the fluctuations expected from cosmic variance, thereby establishing the statistical significance. The SDSS DR4 covers a large contiguous region in the Northern Galactic Cap with a few gaps still to be covered. The SDSS has been carried out in overlapping strips of 5° width oriented along great circles. Since the detection of coherent large-scale features requires a completely sampled region with no gaps, we have extracted seven non-overlapping strips of width 2° each. The volume corresponding to each strip is nearly two dimensional and we have collapsed the thickness and analysed the resulting 2-D galaxy distribution. The increased number of strips provide a better estimate of the cosmic variance leading to more robust conclusions. The analysis has been carried out on five overlapping bins in absolute magnitude. We have extracted separate volume limited subsamples corresponding to each magnitude bin and compared the filamentarity across them. The earlier analysis has been extended here to also consider the colour and morphology dependence, which has been tested in each of the volume limited subsamples.

A brief outline of our paper follows. Section 2 describes the data and Section 3 the method of analysis. Our results are presented in Section 4 and finally we present our conclusions in Section 5.

It may be noted that we have used a Λ CDM cosmological model with $\Omega_{m0} = 0.3$, $\Omega_{\Lambda0} = 0.7$ and $h = 1$ throughout.

2 THE DATA

The SDSS is an imaging and spectroscopic survey of the sky (York et al. 2000) in five photometric bandpasses, u,g,r,i,z with effective wavelengths of 3540\AA , 4760\AA , 6280\AA , 7690\AA and 9250\AA respectively (Fukugita et al. 1996, Smith et al. 2002) to a limiting r band magnitude ~ 22.2 with 95% completeness. A series of pipelines that perform astrometric calibration (Pier et al. 2003), photometric reduction (Lupton et al. 2002) and photometric calibration (Hogg et al. 2001) are used to process the imaging data and then objects are selected from the imaging data for spectroscopy. In the SDSS DR4 (Adelman-McCarthy et al. 2005) the imaging data covers 6670 deg^2 of the sky whereas the spectroscopy covers a total area of 4783 deg^2 . The spectroscopic data includes 673,280 spectra with approximately 480,000 galaxies, 64,000 quasars and 89,000 stars. The survey area covers a single contiguous region in the Northern Galactic Cap and three non-contiguous region in the Southern Galactic Cap. Our analysis is restricted to the Northern Galactic Cap region only.

The samples analyzed here were obtained from the SDSS DR4 Skyserver¹. This is a web interface to the SDSS data archive server. The SDSS surveys the sky in overlapping stripes² of width 5° which form great circles on the sky. The stripes are most conveniently described using survey co-ordinates (λ, η) defined in Stoughton et al. (2002). Lines of constant η are great circles aligned with the stripes and lines of constant λ are small circles along the width of the stripes. Each stripe is centered along a line of constant η separated from the adjoining stripe by 2.5° . We have downloaded data from seven overlapping stripes (Table I) which form a nearly contiguous region shown in Figure 1. We have selected all objects identified as galaxies with extinction corrected r band Petrosian magnitude $r < 17.77$ over the redshift range $0.01 \geq z \geq 0.2$. The number of galaxies satisfying these criteria in each stripe is given in Table I.

The primary data described in Table I is not contiguous and has a few gaps. Since our analysis requires contiguous regions, we have extracted seven non-overlapping strips each of width 2° in η and spanning 90° in λ (Figure 1 and Table II). Only galaxies with extinction corrected Petrosian r band magnitude in the range $14.5 \geq m_r \geq 17.77$ were used. For each galaxy the absolute magnitude was computed using its redshift, apparent magnitude, K correction and reddening correction (Schlegel, Finkbeiner & Davis 1998). We adopt a polynomial fit (Park et al. 2005) for the mean K-correction, $K(z) = 2.3537(z - 0.1)^2 + 1.04423(z - 0.1) - 2.5 \log(1 + 0.1)$.

We construct volume limited sub-samples using the absolute magnitude bins listed in Table III. The five overlapping

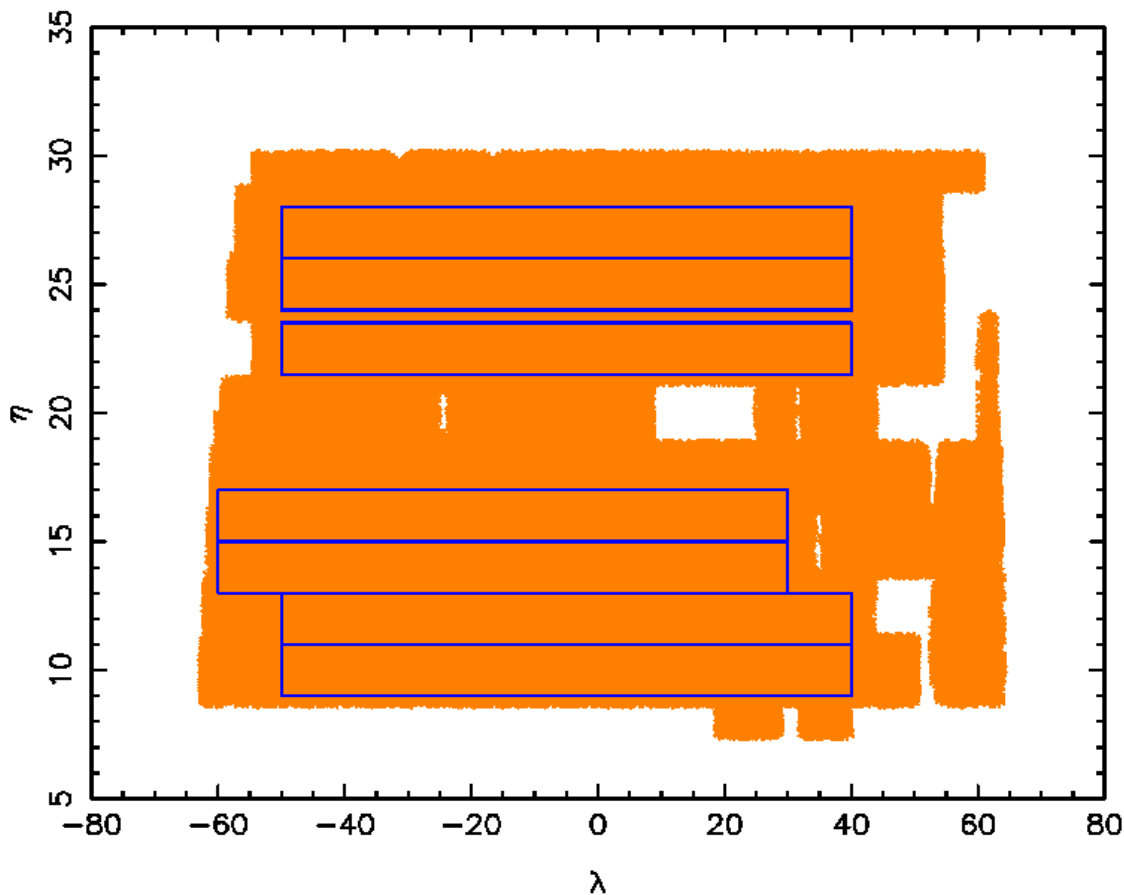
¹ (<http://cas.sdss.org/dr4/en/>)

² <http://www.sdss.org/dr4/coverage/atStripeDef.par>

Table I

Table 1. This shows parameters of the seven SDSS stripes which constitute our primary data. The Stripe number are those used in the survey and (λ, η) are the survey coordinates.

Stripe number	λ_{min}	λ_{max}	Span in η	No. of galaxies
27	-62.3°	63.7°	$(10 \pm 2.5)^\circ$	31635
28	-61.8°	63.6°	$(12.5 \pm 2.5)^\circ$	37541
29	-61.2°	63.4°	$(15 \pm 2.5)^\circ$	37543
30	-60.6°	63.1°	$(17.5 \pm 2.5)^\circ$	35461
32	-58.9°	62.4°	$(22.5 \pm 2.5)^\circ$	34431
33	-57.8°	61.9°	$(25 \pm 2.5)^\circ$	38389
34	-56.6°	61.2°	$(27.5 \pm 2.5)^\circ$	38106

**Figure 1.** The shaded part shows the contiguous region covered by the seven overlapping strips described in Table I. The bounded regions within show the seven 2° wide non-overlapping strips used in our analysis.

absolute magnitude bins are referred to as “bin 1”, “bin 2”, ... “bin 5” in order of increasing luminosity. Each bin extends over a different redshift range as listed in Table III. The galaxy number density falls considerably for galaxies brighter than M^* which has a value $M^* = -20.44 \pm 0.01$ (Blanton et al. 2003) for the SDSS. The absolute magnitude interval of bin 1, which is fainter than M^* , is smaller to optimize the redshift range maintaining a nearly equal galaxy number density for all the bins. The thickness of the volume corresponding to each bin increases with redshift. We have extracted regions of uniform thickness $6 h^{-1}$ Mpc which corresponds to 2° at redshift 0.06. For some bins it was necessary to discard a part of the low redshift region where the thickness was less than $6 h^{-1}$ Mpc. For each strip, the number of galaxies in each bin is tabulated in Table II.

To study the luminosity dependence it is necessary to compare the galaxy distribution in identical volumes with the same galaxy number density in different luminosity bins. The faintest subsample (bin 1) occupies the smallest volume. We have

Table II

Table 2. This shows the (λ, η) range of the seven non-overlapping strips extracted from the primary data. For each strip the table shows the number of galaxies in volume limited subsamples bin 1, bin 2, .. etc. with absolute magnitude and redshift limits given in Table III.

Strip number	λ	η	bin 1	bin 2	bin 3	bin 4	bin 5
1	$-50 \leq \lambda \leq 40$	$9 \leq \eta \leq 11$	875	2016	2108	1943	1623
2	$-50 \leq \lambda \leq 40$	$11 \leq \eta \leq 13$	839	1740	1780	1695	1591
3	$-60 \leq \lambda \leq 30$	$13 \leq \eta \leq 15$	663	1492	1665	1597	1540
4	$-60 \leq \lambda \leq 30$	$15 \leq \eta \leq 17$	678	1547	1629	1569	1593
5	$-50 \leq \lambda \leq 40$	$21.5 \leq \eta \leq 23.5$	846	1878	1863	1703	1595
6	$-50 \leq \lambda \leq 40$	$24 \leq \eta \leq 26$	782	1905	1854	1839	1668
7	$-50 \leq \lambda \leq 40$	$26 \leq \eta \leq 28$	648	1550	1573	1692	1633

Table III

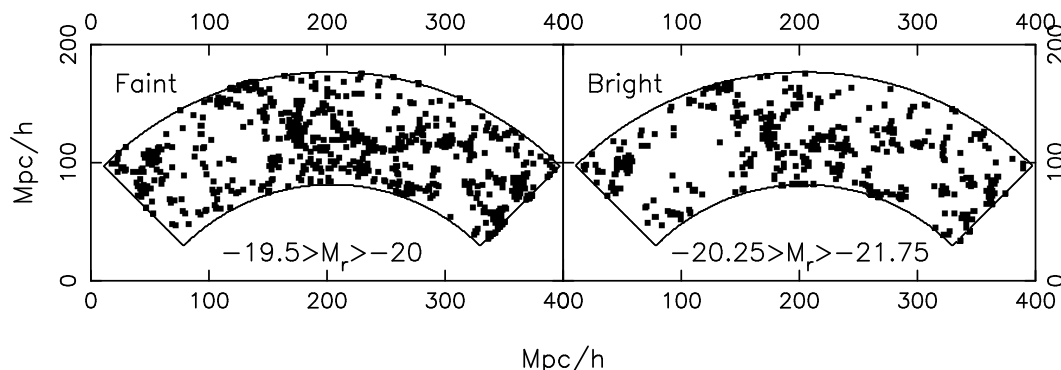
Table 3. This shows the absolute magnitude and redshift limits for the different volume limited subsamples analysed.

bin	Absolute Magnitude range	Redshift range
bin 1	$-19.5 \geq M_r \geq -20$	$0.028 \leq z \leq 0.093$
bin 2	$-19.75 \geq M_r \geq -21.25$	$0.048 \leq z \leq 0.103$
bin 3	$-20 \geq M_r \geq -21.5$	$0.054 \leq z \leq 0.114$
bin 4	$-20.25 \geq M_r \geq -21.75$	$0.06 \leq z \leq 0.126$
bin 5	$-20.5 \geq M_r \geq -22$	$0.067 \leq z \leq 0.14$

extracted volumes identical to bin 1 from all the other bins. Further, we allow a (5 – 10)% variation in the number of galaxies across the bins, and randomly chosen galaxies were discarded from the bins containing considerably excess galaxies. We have verified that variation in the number density by around $\sim 50\%$ does not cause a statistically significant change in our results. Figure 2 shows the galaxy distribution in two different luminosity bins drawn from the same strip.

To study the colour dependence we separately consider each magnitude bin listed in Table II and Table III, we do not study colour dependence across the bins. For each bin the galaxies are divided into two halves based on their $u - r$ colours which has been found to have a bimodal distribution (Strateva et al. 2001). In our analysis the cutoff $(u - r)_c$ is chosen so that it divides each magnitude bin into equal number of red (i.e. $u - r > (u - r)_c$) and blue (i.e. $u - r \leq (u - r)_c$) galaxies. The value of $(u - r)_c$ varies slightly across the bins, and the values are listed in Table IV. It may be noted that Strateva et al. (2001) finds that a color selection criteria $(u - r)_c = 2.22$ ensures that the red galaxies are ‘ellipticals’ with 90% completeness. Figure 3 shows the distribution of red and blue galaxies in one of the subsamples.

The morphological classification was carried out using the concentration index defined as $c_i = r_{90}/r_{50}$ where r_{90} and r_{50} are the radii containing 90% and 50% of the Petrosian flux respectively. This has been found to be one of the best parameter to classify galaxy morphology (Shimasaku et al. 2001). Ellipticals are expected to have a larger concentration indices than spirals. It was found that $c_i \simeq 3.33$ for a pure de-Vaucouleurs profile (Blanton et al. 2001) while $c_i \simeq 2.3$ for a pure exponential profile (Strateva et al. 2001). Strateva et al. (2001) show that using a cutoff $c_{i,c} = 2.6$ divides the sample into ellipticals and spirals at 83% completeness. For each bin listed in Table II and Table III we have chosen a cutoff $c_{i,c}$ such that it divides the


Figure 2. This shows the distribution of faint and bright galaxies in one of the strips in magnitude bin 1 and bin 4 respectively after three round of coarse-graining.

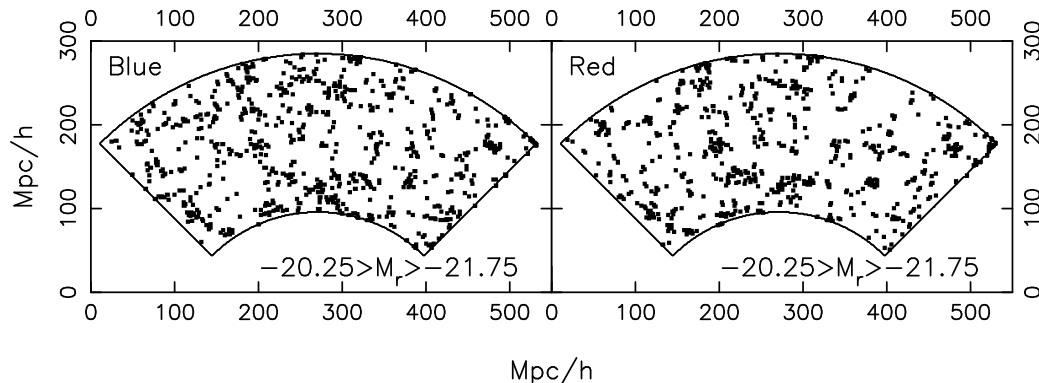


Figure 3. This shows the distribution of blue and red galaxies in one of the strips in magnitude bin 4 after three round of coarse-graining.

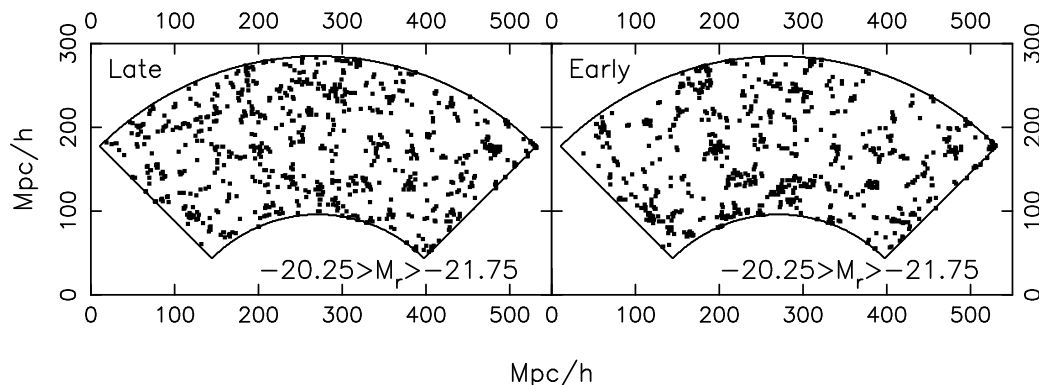


Figure 4. This shows the distribution of early and late type galaxies in one of the strips in magnitude bin 4 after three round of coarse-graining.

sample into two equal parts, one predominantly ellipticals and the other spirals. The values of $c_{i,c}$ varies across bins and are listed in Table IV. We have tested for morphology dependence separately in each magnitude bin, and we have not tested for morphology dependence across bins. Figure 4 shows the distribution of early and late type galaxies in one of the subsamples.

3 METHOD OF ANALYSIS

Each of the subsamples described in the previous subsection have a much greater (16-35 times) linear dimension compared to their thickness and so can be reasonably treated as two dimensional. The 2D galaxy distribution was embedded in a $1 h^{-1}\text{Mpc} \times 1 h^{-1}\text{Mpc}$ 2D rectangular grid. The galaxy distribution was represented as a set of 1s and 0s on a 2-D rectangular grid by assigning the values 1 and 0 to the filled and empty cells respectively. The grid cells which are beyond the boundaries of the survey were assigned a negative value in order to distinguish them from the empty cells within the survey area.

The next step is to use an objective criteria to identify the coherent large-scale structures visible in the galaxy distribution. We use a “friends-of-friends”(FOF) algorithm to identify interconnected regions of filled cells which we refer to as clusters. In this algorithm any two adjacent filled cells are referred to as friends. Clusters are defined through the stipulation that any

Table IV

Table 4. For each volume limited subsample this shows the value of the galaxy colour $(u-r)_c$ and the value of the concentration index $c_{i,c}$ used to divide the data into equal numbers of red/blue and elliptical/spiral galaxies respectively.

bin	$(u-r)_c$	$c_{i,c}$
bin1	2.14	2.53
bin2	2.35	2.67
bin3	2.41	2.72
bin4	2.45	2.75
bin5	2.5	2.78

friend of my friend is my friend. The distribution of 1s on the grid is very sparse with only $\sim 1\%$ of the cells being filled. Also, the filled cells are mostly isolated, and the clusters identified using FOF, which contain only a few cells each, do not resemble the large-scale coherent structures seen in the SDSS strips. It is necessary to coarse-grain the galaxy distribution so that the large scale structures may be objectively identified. The coarse-graining is carried out by gradually making each filled cell fatter until the filled cells overlap and they finally fill up the whole survey area. In every iteration of coarse-graining we fill up all the empty cells which are adjacent to filled cells, causing every filled cell to grow fatter. This causes clusters to grow, first because of the growth of filled cells, and then by the merger of adjacent clusters as they overlap. At the initial stages of coarse-graining, the patterns which emerge from the distribution of 1s and 0s closely resembles the coherent structures seen in the galaxy distribution. As the coarse-graining proceeds, the clusters become very thick and fill up the entire region washing away any visibly distinct pattern. The filling factor FF, defined as the fraction of cells within the survey area that are filled, *ie.*

$$\text{FF} = \frac{\text{Total No. of Filled Cells}}{\text{Total No. of Cells Inside the Survey Area}} \quad (1)$$

increases from $\text{FF} \sim 0.01$ to $\text{FF} = 1$ as the coarse graining proceeds. So as to not restrict our analysis to an arbitrarily chosen level of smoothing, we analyze the clusters identified in the pattern of 1s and 0s after each iteration of coarse-graining *ie.* the whole range of FF.

The geometry and topology of a two dimensional cluster can be described by the three Minkowski functionals, namely its area S , perimeter P , and genus G . It is possible to quantify the shape of the cluster using a single 2D ‘‘Shapefinder’’ statistic (Bharadwaj et al. 2000) which is defined as the dimensionless ratio

$$\mathcal{F} = \frac{P^2 - 4\pi S}{P^2 + 4\pi S}, \quad (2)$$

which by construction has values in the range $0 \leq \mathcal{F} \leq 1$. It can be verified that $\mathcal{F} = 1$ for an ideal filament which has a finite length and zero width, whereby it subtends no area ($S = 0$) but has a finite perimeter ($P > 0$). It can be further checked that $\mathcal{F} = 0$ for a circular disk, and intermediate values of \mathcal{F} quantifies the degree of filamentarity with the value increasing as a cluster is deformed from a circular disk to a thin filament.

The definition of \mathcal{F} needs to be modified when working on a rectangular grid of spacing l . An ideal filament, represented on a grid, has the minimum possible width *ie.* l , and its perimeter P and area S are related as $P = 2S + 2l$. At the other extreme we have $P^2 = 16S$ for a square shaped cluster on the grid. We introduce the 2D Shapefinder statistic

$$\mathcal{F} = \frac{(P^2 - 16S)}{(P - 4l)^2} \quad (3)$$

to quantify the shape of clusters on a grid. By definition $0 \leq \mathcal{F} \leq 1$. \mathcal{F} quantifies the degree of filamentarity of the cluster, with $\mathcal{F} = 1$ indicating a filament and $\mathcal{F} = 0$, a square, and \mathcal{F} changes from 0 to 1 as a square is deformed to a filament.

The extent of filamentarity in a survey is mostly dominated by the morphology of the most massive members as a large cluster has a greater contribution to the overall texture of large-scale structure than an individual galaxy. We therefore want to give greater weight to larger objects and used the second moment of filamentarity as the indicator of average filamentarity. The average filamentarity F_2 is defined as the mean filamentarity of all the clusters in a slice weighted by the square of the area of each clusters

$$F_2 = \frac{\sum_i S_i^2 \mathcal{F}_i}{\sum_i S_i^2}. \quad (4)$$

In the current analysis, we study the average filamentarity F_2 as a function of FF to quantify the degree of filamentarity in each of the SDSS subsamples and investigate how the average filamentarity F_2 changes with intrinsic galaxy properties like luminosity, color and morphology.

At a specified level of coarse-graining the value of the filling factor (FF) differs from sample to sample. This makes it difficult to compare the filamentarity in different samples using the values of the average filamentarity (F_2) as a function of FF . We overcome this by interpolating the values of F_2 as a function of FF at uniformly chosen values which are same for all the samples.

4 RESULTS

We first study how the average filamentarity varies across the different luminosity bins discussed in Section 2. For each luminosity bin we have seven independent realisations of the galaxy distributions from the seven non-overlapping strips. For each bin we use the results from these seven samples to determine the mean and variance of F_2 at uniformly chosen values of FF . The results are shown in Figure 5. We find that for a fixed value of FF , the value of F_2 decreases with increasing luminosity. We note that there is some deviation from this behaviour at $FF > 0.4$ between bins 3 and 4, but the overall trend

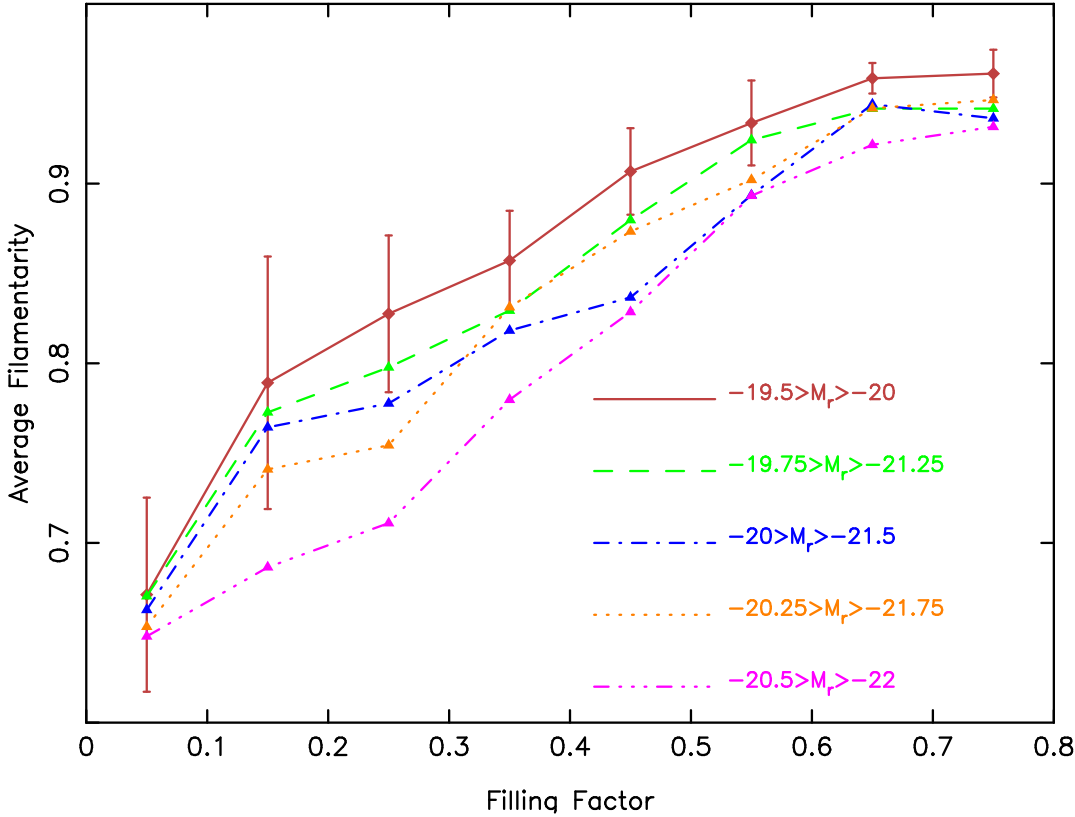


Figure 5. This shows the average filamentarity (F_2) as a function of filling factor (FF) for the galaxies in different luminosity bins. The $1 - \sigma$ errorbars for the faintest sample is shown in the figure which shows variation from sample to sample. The error bars are very similar for the other luminosity bins.

is still valid when we compare these bins with fainter or brighter samples. Further, the luminosity dependence is enhanced with increasing luminosity.

At each values of FF we use the Student's t-test to quantify the statistical significance of the difference in the mean F_2 between different luminosity bins. The variance of F_2 is very similar in the different luminosity bins and we estimate the standard error for the difference in the means using

$$s_D = \sqrt{\frac{\sum_{i \in A} (x_i - \bar{x}_A)^2 + \sum_{i \in B} (x_i - \bar{x}_B)^2}{N_A + N_B - 2}} \left(\frac{1}{N_A} + \frac{1}{N_B} \right)$$

where the sum is over the points in the two samples A and B which are being compared. Here \bar{x}_A and \bar{x}_B refers to the mean, and N_A and N_B refers to the number of data points. In our case $N_A = N_B = 7$. We use $t = \frac{\bar{x}_A - \bar{x}_B}{s_D}$ to estimate the significance of the differences in the means. This is expected to follow a Student's t-distribution with 12 degrees of freedom. We accept the difference in the means as being statistically significant if the probability of its occurring by chance is less than 5%. We find that there are no statistically significant differences between adjacent luminosity bins except the two brightest ones (bins 4 and 5). All the non-adjacent bins (eg. bin 1 and bin 3, etc.) show statistically significant differences at most values of FF .

We have separately analyzed the filamentarity of the red and blue galaxies in each luminosity bin. The results for bin 4 are shown in figure 6. We find that there is a statistically significant colour dependence. The red galaxies exhibit a higher filamentarity at the smallest value of FF , whereas the blue galaxies have a larger filamentarity at other values of FF . A similar trend is found in all the other luminosity bins, results for which have not been shown here.

The morphology dependence has been studied separately for each luminosity bin. The results are shown in figure 7 for bin 4. The ellipticals have a higher F_2 for $FF \leq 0.25$ whereas the spirals have a larger F_2 at higher values of FF . We find that the differences are statistically significant for $FF \leq 0.1$ and $FF \geq 0.4$. The results are similar for the other luminosity bins not shown here.

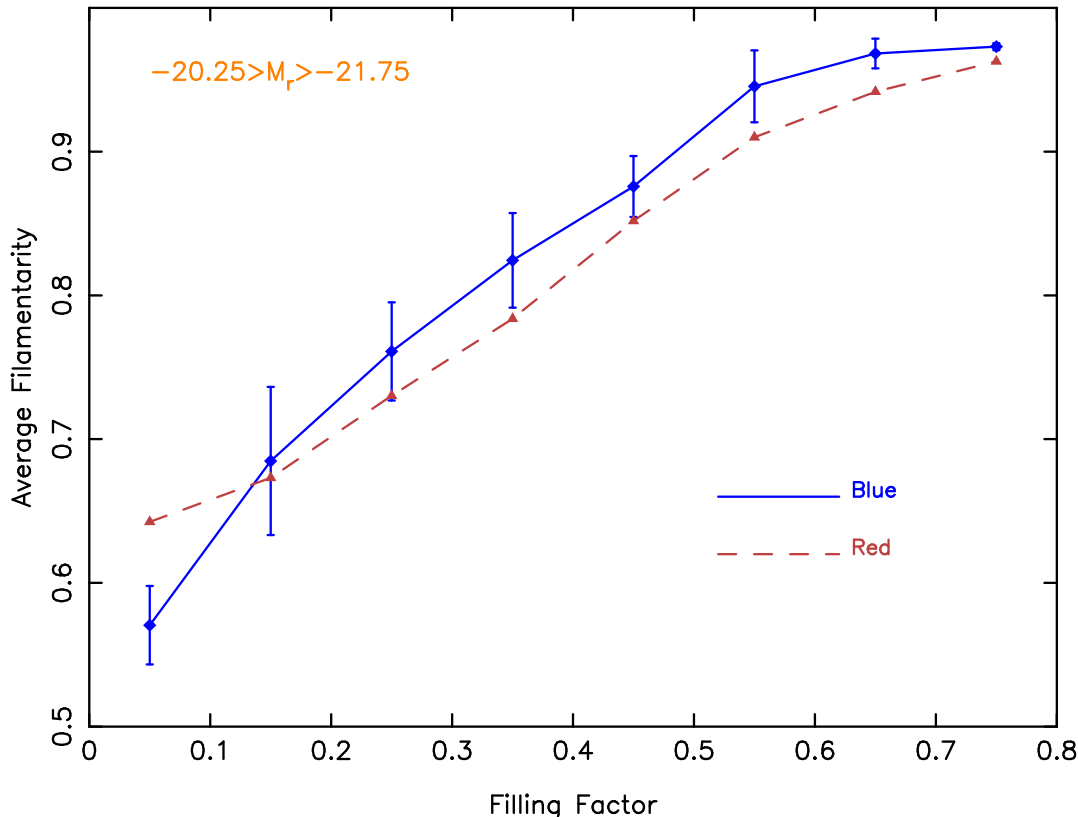


Figure 6. This shows the average filamentarity (F_2) as a function of filling factor (FF) for the red and blue galaxies in magnitude bin 4. The 1σ error bars for blue galaxies shows sample to sample variation in the data. The 1σ error bars are of same size for the red galaxies.

5 DISCUSSION AND CONCLUSION

Filaments are the largest known statistically significant coherent features visible in the galaxy distribution. We test if the degree of filamentarity depends on the galaxy properties. Performing the analysis at different levels of coarse graining allows us to address this issue at different lengthscales. We find evidence for statistically significant luminosity, colour and morphology dependence in the average filamentarity F_2 studied as a function of the filling factor FF . We find that the differences exist at nearly all values of FF . It may be noted that FF increases with every iteration of coarse graining.

The brighter galaxies are found to have a less filamentary distribution at all values of FF . The effect is more pronounced for galaxies brighter than M^* . Our analysis indicates that galaxies of different luminosity are not uniformly distributed along the cosmic web. While the faint galaxies are distributed along the filaments, the bright ones are found in less filamentary regions, possibly the nodes where the filaments intersect. The luminosity segregation extends to lengthscales comparable to the largest scales at which the filaments themselves are statistically significant. We note that studies using the projected two-point correlation function (eg. Norberg et al. 2002; Zehavi et al. 2005) show that the correlation amplitude increases with luminosity, the effect being pronounced beyond L^* . Recent studies (eg. Coil et al. 2005; Pollo et al. 2005) show evidence for luminosity dependence at higher redshifts ($z \simeq 1$) also.

The results for colour and morphology dependence are somewhat different from those for luminosity dependence. We find that the red galaxies and the ellipticals have a higher filamentarity at low filling factors. There is a cross-over at $FF \sim 0.15$ for the colour dependence and $FF \sim 0.25$ for the morphology dependence. The blue galaxies and the spirals have higher filamentarity at large filling factors. It may be noted that the colour and morphology are very strongly correlated galaxy properties, the red galaxies being predominantly ellipticals and the blue ones spirals. The colour and morphology are also known to be correlated with the luminosity, the red galaxies being more luminous.

Our results for the colour and morphology dependence of the filamentarity may be interpreted in terms of an interconnected network of filaments (the Cosmic Web) where the ellipticals densely populate the nodes and extend a little along the filaments which originate from the nodes, while the spirals are distributed along the entire extent of the filaments. This is shown schematically in Figure 8. In this picture the ellipticals have a more compact distribution which connects up to form filamentary clusters at a low level of coarse-graining. These structures do not grow much as the coarse graining proceeds. On the other hand, the spirals are sparsely distributed and connect up at a later stage of coarse graining to define the entire filamentary network of the Cosmic Web.

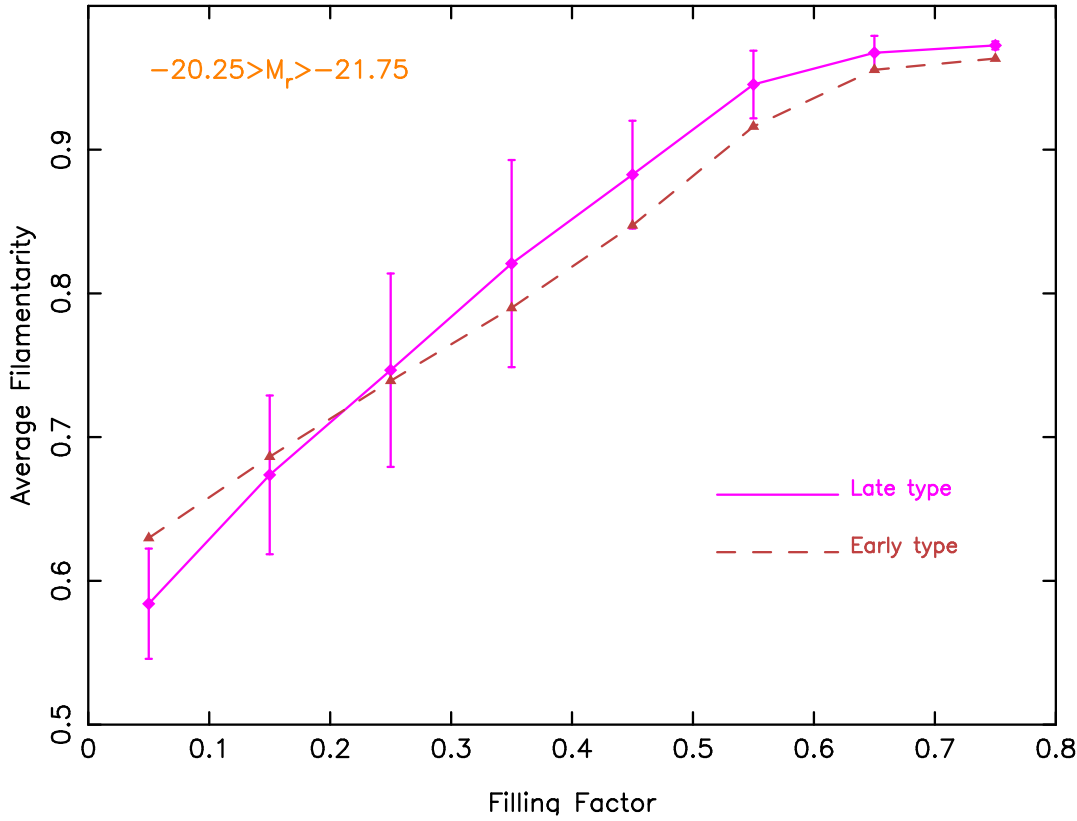


Figure 7. This shows the average filamentarity (F_2) as a function of filling factor (FF) for the early type ellipticals and late type spirals in magnitude bin 4. The $1 - \sigma$ errorbars for late type galaxies are shown in the figure which are of same size for the early types.

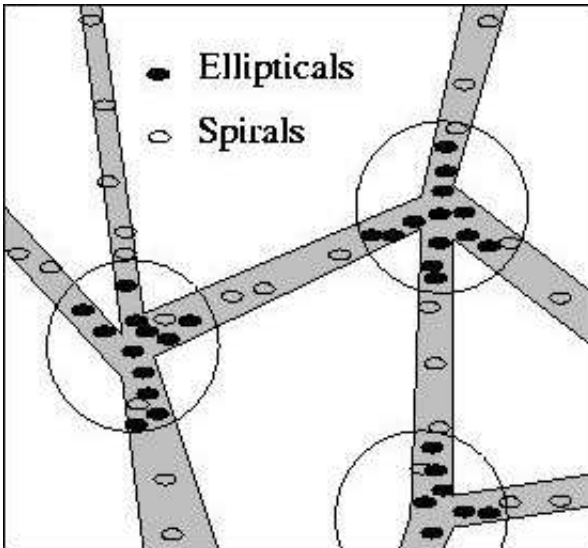


Figure 8. This shows our picture for the relative distribution of ellipticals and spirals along the Cosmic Web. The ellipticals densely inhabit the nodes and are distributed within the encircled regions shown in the figure. The spirals are sparsely distributed along the larger volume of the entire filaments.

Observational findings indicate a close connection between the local density and galaxy type (Dressler 1980) with an increase in the elliptical and S0 population and a decrease in the spirals in galaxy clusters. Our findings are consistent with this, and it indicates that there is an excess of ellipticals on scales larger than the clusters extending into the filaments. In the Zel'dovich pancake scenario filaments form at the intersection of sheets and clusters form at the nodes of the filaments. Structure formation occurs in a hierarchical fashion with sheets forming first, matter flows along the sheets into the filaments

which in turn drain into the clusters. The higher galaxy density and a denser hot gas environment are possibly the factors leading to a higher elliptical fraction in the vicinity of the nodes.

The relation between our findings and the various theories for galaxy formation is an important issue which we propose to address in future. The SDSS data now covers a significantly large volume. It is now meaningful to carry out a three dimensional analysis which we propose to address in future work.

6 ACKNOWLEDGMENT

SB would like to acknowledge financial support from the Govt. of India, Department of Science and Technology (SP/S2/K-05/2001). BP would like to thank the CSIR, Govt. of India for financial support through a Senior Research Fellowship. The SDSS DR4 data was downloaded from the SDSS skyserver <http://skyserver.sdss.org/dr4/en/>.

Funding for the creation and distribution of the SDSS Archive has been provided by the Alfred P. Sloan Foundation, the Participating Institutions, the National Aeronautics and Space Administration, the National Science Foundation, the U.S. Department of Energy, the Japanese Monbukagakusho, and the Max Planck Society. The SDSS Web site is <http://www.sdss.org/>.

The SDSS is managed by the Astrophysical Research Consortium (ARC) for the Participating Institutions. The Participating Institutions are The University of Chicago, Fermilab, the Institute for Advanced Study, the Japan Participation Group, The Johns Hopkins University, the Korean Scientist Group, Los Alamos National Laboratory, the Max-Planck-Institute for Astronomy (MPIA), the Max-Planck-Institute for Astrophysics (MPA), New Mexico State University, University of Pittsburgh, Princeton University, the United States Naval Observatory, and the University of Washington.

REFERENCES

- Abazajian, K., et al. 2003, AJ, 126, 2081
Abazajian, K., et al. 2004, AJ, 128, 502
Adelman-McCarthy, J.K., et al. 2005, astro-ph/0507711
Basilakos, S., Plionis, M., & Rowan-Robinson, M. 2001, MNRAS, 323, 47
Benoist, C., Maurogordato, S., da Costa, L.N., Cappi, A., & Schaeffer, R., 1996, ApJ, 472, 452
Benson et al. 2000, MNRAS, 311, 793
Berlind, A., Weinberg, D.H. 2002, ApJ, 575, 587
Bharadwaj, S., Sahni, V., Sathyaprakash, B. S., Shandarin, S. F., & Yess, C. 2000, ApJ, 528, 21
Bharadwaj, S., Bhavsar, S. P., & Sheth, J. V. 2004, ApJ, 606, 25
Bharadwaj, S., Pandey, B. 2004, ApJ, 615,1
Blanton, M. R., et al. 2003, ApJ, 594, 186
Blanton, M. R., et al. 2001, AJ, 121, 2358
Blanton, M. R., et al. 2003, ApJ, 592, 819
Brown, M.J.I., Webster, R.L., & Boyle, B.J., 2000, MNRAS,317, 782
Coil, A.L., Newman, J.A., Cooper, M.C., Davis, M., Faber, S.M., Koo, D.C., Willmer, C.N.A., 2005, submitted to ApJ, (astro-ph/ 0512233)
Colles, M. et al.(for 2dFGRS team) 2001,MNRAS,328,1039
Corray, A., Sheth, R.K., 2002, Phys. Rep., 371, 1
Davis, M., Meiksin, A., Strauss, M.A., da Costa, L.N., & Yahil, A., 1988, ApJ, 333, L9
Davis, M., & Geller, M.J., 1976, ApJ, 208, 13
Davis, M., Efstathiou, G., Frenk, C.S., White, S.D.M., 1985, ApJ, 292, 371
Doroshkevich, A. G., Tucker, D. L., Fong, R., Turchaninov, V., & Lin, H. 2001, MNRAS, 322, 369
Doroshkevich, A., Tucker, D. L., Allam, S., & Way, M. J. 2004, A&A, 418,7
Dressler, A., 1980, ApJ, 236, 351
Einasto, J., Klypin, A. A., Saar, E., & Shandarin, S. F. 1984, MNRAS, 206, 529
Einasto, J., Hütsi, G., Einasto, M., Saar, E., Tucker, D. L., Müller, V., Heinämäki, P., & Allam, S. S. 2003, A&A, 405, 425
Fukugita, M., Ichikawa, T., Gunn, J. E., Doi, M., Shimasaku, K., & Schneider, D. P. 1996, AJ, 111, 1748
Geller, M.J. & Huchra, J.P.1989, Science,246,897
Goto, T., Yamauchi, C., Fujita, Y., Okamura, S., Seikiguchi, M., Smail, I. Bernardi, M., & Gomez, P.L., 2003, MNRAS, 346, 601
Guzzo, L., Strauss, M.A., Fisher, K.B., Giovanelli, R., & Haynes, M.P., 1997, ApJ, 489, 37
Gaztañaga, E., Norberg, P., Baugh, C. M., & Croton, D. J. 2005, MNRAS, 364, 620
Hogg, D. W., Finkbeiner, D. P., Schlegel, D. J., & Gunn, J. E. 2001, AJ, 122, 2129
Hogg, D. W., et al. 2003, ApJL, 585, L5

- Hoyle, F., et al. 2002, ApJ, 580, 663
- Hamilton, A.J.S., 1988, ApJ, 331, L59
- Hubble, E.P., 1936, *The Realm of the Nebulae* (Oxford University Press: Oxford), 79
- Jing, Y.P., Mo, H.J., Borner, G. 1998, ApJ, 494,1
- Jing, Y. P.,Borner, G. 2004, ApJ, 607, 140
- Kolokotronis, V., Basilakos, S., & Plionis, M. 2002, MNRAS, 331, 1020
- Kaiser, N. 1984, ApJL, 284, L9
- Kayo, I., et al. 2004, *Publications of the Astronomical Society of Japan*, 56, 415
- Lupton, R. H., Ivezić, Z., Gunn, J. E., Knapp, G., Strauss, M. A., & Yasuda, N. 2002, *Proceedings of the SPIE*, 4836, 350
- Loveday, J., Maddox, S.J., Efstathiou, G., & Peterson, B.A. , 1995, ApJ, 442, 457
- Ma, C.P., Fry, J.N. 2000, ApJ, 543, 503
- Müller, V., Arbabi-Bidgoli, S., Einasto, J., & Tucker, D. 2000, MNRAS, 318, 280
- Norberg, P., et al. 2001, MNRAS, 328, 64
- Norberg, P., et al. 2002, MNRAS, 332, 827
- Pandey, B. & Bharadwaj, S. 2005, MNRAS, 357, 1068
- Park, C., Vogeley, M.S., Geller, M.J., & Huchra, J.P., 1994, ApJ, 431,569
- Park, C., et al. 2005, ApJ, 633, 11
- Peebles, P.J.E., Phelps, S.D., Shaya, E.J., & Tully, R.B., 2001, ApJ, 554, 104
- Peacock J.A., Smith, R.E. 2000, MNRAS, 318, 1144
- Pier, J. R., Munn, J. A., Hindsley, R. B., Hennessy, G. S., Kent, S. M., Lupton, R. H., & Ivezić, Ž. 2003, AJ, 125, 1559
- Pimblet, K. A., Drinkwater, M. J., & Hawkrigg, M. C. 2004, MNRAS, 354, L61
- Pollo, A., Guzzo, L., Le Fevre, O., Meneux, B., the VVDS team, 2005, submitted to A&A,(astro-ph/0512429)
- Ratcliffe, A., Shanks, T., Broadbent, A., Parker, Q.A., Watson, F.G., Oates, A.P., Fong, R., & Collins, C.A., 1996, MNRAS, 281, L47
- Sheth, J. V., Sahni, V., Shandarin, S. F., & Sathyaprakash, B. S. 2003, MNRAS, 343, 22
- Sheth,J.V., 2003, MNRAS, Submitted, astro-ph/0310755
- Shandarin, S. F. & Zeldovich, I. B. 1983, *Comments on Astrophysics*, 10, 33
- Shandarin, S. F. & Yess, C. 1998, ApJ, 505, 12
- Shectman, S. A.,Landy, S. D., Oemler, A., Tucker, D. L., Lin, H., Kirshner, R. P., & Schechter, P. L. 1996, ApJ, 470, 172
- Schechter, P., 1976, ApJ, 203, 297
- Smith, J. A., et al. 2002, AJ, 123, 2121
- Stoughton, C., et al. 2002, AJ, 123, 485
- Schlegel, D.J., Finkbeiner, D.P., & Davis, M., 1998, ApJ, 500,525
- Strateva, I., et al. 2001, AJ, 122, 1861
- Shimasaku, K., et al. 2001, AJ, 122, 1238
- Seljak, U. 2000, MNRAS, 318, 203
- Soccimarro, R., Sheth, R. 2001, ApJ, 329, 629
- Scranton, R. 2002, MNRAS, 332, 697
- Trac, H., Mitsouras, D., Hickson, P., & Brandenberger, R. 2002, MNRAS, 330, 531
- Willmer, C.N.A., da Costa, L.N., & Pellegrini, P.S., 1998, AJ, 115, 869
- White, S.D.M., Tully, R.B., & Davis, M., 1988, ApJ, 333, L45
- White, S.D.M., Davis, M., Efstathiou, G., Frenk, C.S., 1987, *Nature*, 330, 351
- Yang, X., Mo, H.J., van den Bosch, F.C. 2003, MNRAS, 339, 1057
- Yang, X., Mo, H.J., Jing, Y.P., van den Bosch, F.C. 2005, MNRAS, 358, 217
- York, D. G., et al. 2000, AJ, 120, 1579
- Zehavi, I., et al. 2002, ApJ,571,172
- Zehavi, I., et al. 2005, ApJ, 630, 1
- Zel'dovich, I. B., Einasto, J., & Shandarin, S. F. 1982, *Nature*, 300, 407
- Zwicky, F., Herzog, E., Wild, P., Karpowicz, M., & Kowal, C., 1961-1968, *Catalog of Galaxies and Clusters of Galaxies*, vols. 1-6 (Pasadena: California Institute of Technology)